

# QWEST and HyTES: Two New Hyperspectral Thermal Infrared Imaging Spectrometers for Earth Science

Simon J. Hook<sup>1</sup>, Bjorn T. Eng, Sarath D. Gunapala, Cory J. Hill, William R. Johnson, Andrew U. Lamborn, Pantazis Mouroulis, Jason M. Mumolo, Christopher G. Paine, Vincent J. Realmuto, Daniel W. Wilson

Jet Propulsion Laboratory  
California Institute of Technology  
Pasadena, California 91109

Tel: 818-354-09741

Fax: 818-354-5148

Email: [Simon.J.Hook@jpl.nasa.gov](mailto:Simon.J.Hook@jpl.nasa.gov)

*Abstract*— We have recently developed a laboratory prototype of an airborne thermal infrared imaging spectrometer termed the Quantum Well Earth Science Testbed (QWEST). Based on our experience with QWEST we have started to develop the airborne Hyperspectral Thermal Emission Spectrometer (HyTES). HyTES is scheduled for completion in 2011. Both instruments utilize several key components: slits, spectrometers, gratings and detectors developed at the Jet Propulsion Laboratory. In particular, each design uses a Dyson spectrometer, an electron microbeam grating and a Quantum Well Infrared Photodetector (QWIP) focal plane array. The Dyson configuration uses a single monolithic prism-like grating design which allows for a high throughput instrument (F/1.6) with minimal ghosting, stray-light and large swath width. The configuration has the potential to be the optimal imaging spectroscopy solution for lighter-than-air (LTA) vehicles, unmanned aerial vehicles (UAV), manned airborne platforms and spaceborne platforms due to its small form factor and relatively low power requirements. The instrument specifications will be discussed as well as design trade-offs. Calibration results from QWEST (noise equivalent temperature difference, spectral linearity and spectral bandwidth) will be presented as well as some field results. Field testing of QWEST was performed to acquire data from a variety of standard minerals and these will be compared to laboratory measurements of the same minerals made with an FTIR spectrometer.

## Table of Contents

1. INTRODUCTION.....	1
2. OPTICAL DESIGN .....	2
3. THE QWIP ARRAY .....	3
4. DIFFRACTION GRATING .....	3
5. SYSTEM SPECIFICATIONS AND RESULTS.....	4
6. REMARKS.....	6
7. ACKNOWLEDGEMENTS .....	7
REFERENCES .....	7

## 1. INTRODUCTION

The Jet Propulsion Laboratory (JPL) has a long history in developing science-grade imaging spectrometers for remote sensing applications. Examples include the airborne visible infrared imaging spectrometer<sup>1</sup> (AVIRIS) and more recently a compact Offner type imaging spectrometer called the Moon Mineralogical Mapper<sup>2</sup> (M<sup>3</sup>) now in orbit around the moon onboard India's Chandrayaan-1.

In late 2006, JPL began the development of a breadboard thermal infrared spectrometer named the Quantum Well Earth Science Testbed (QWEST) as an end to end laboratory demonstration of both the thermal Dyson spectrometer as well as the Quantum Well Infrared Photodetector (QWIP) focal plane technology. The testbed is a precursor to the airborne version under development referred to as the hyperspectral thermal emission spectrometer (HyTES) and funded by the NASA Instrument Incubator Program (IIP). The current effort brings together numerous in-house specialties such as optical design and general spectrometer alignment optimization, precision slit fabrication, high efficiency and low scatter concave diffraction grating design and fabrication, precision mechanical and machining capability and QWIP focal plane arrays.

The long wave infrared (LWIR) is typically expressed as the wavelength range between 7 and 14  $\mu\text{m}$ . Our current demonstration instrument operates between 8-9  $\mu\text{m}$  and the planned airborne instrument will operate between 7.5 and 12  $\mu\text{m}$ . Spectral information from this wavelength range is extremely valuable for Earth Science research. The airborne instrument will be used in support of the HypsIRI mission that was recently recommended by the National Research Council in their Decadal Survey. The LWIR component of the HypsIRI mission will address science questions in five main science themes:

## Volcanoes

What are the changes in the behavior of active volcanoes? Can we quantify the amount of material released into the atmosphere by volcanoes and estimate its impact on Earth's climate? How can we help predict and mitigate volcanic hazards?

## Wildfires

What is the impact of global biomass burning on the terrestrial biosphere and atmosphere, and how is this impact changing over time?

## Water Use and Availability

As global freshwater supplies become increasingly limited, how can we better characterize trends in local and regional water use and moisture availability to help conserve this critical resource?

## Urbanization

How does urbanization affect the local, regional and global environment? Can we characterize this effect to help mitigate its impact on human health and welfare?

## Land surface composition and change

What is the composition and temperature of the exposed surface of the Earth? How do these factors change over time and affect land use and habitability?

The QWEST testbed is providing enabling technology for the development of a fully operational airborne platform suitable for earth science studies. It will have sufficient spatial and spectral resolution to allow scientists to acquire the necessary data to aid in the planning future spaceborne missions.

## 2. OPTICAL DESIGN

Concentric designs allow a point to be mapped perfectly to a focal plane array. Past and future planned imaging spectrometer systems have successfully implemented the Offner<sup>3,4</sup> design. The idea behind the Offner concentric design was to provide a relay unit magnifier to alleviate distortion and third order system aberrations while having an accessible object and image plane. The first published supplementary idea for an all reflecting or 2-mirror concentric imaging spectrometer was cast by Thevenon and Mertz<sup>5</sup>. Subsequent work was also done by Kwo<sup>6</sup> and Lobb<sup>7</sup>. A concentric design like the Offner is well-suited to pushbroom spectrometers. Smile and keystone distortion are nearly eliminated using proper alignment and design techniques.

Although an excellent performer, for the TIR the Offner design would be relatively large and would require a bulky temperature controlled dewar and large power supplies to maintain adequate thermal control. J. Dyson<sup>8</sup> published a paper in 1959 outlining a Seidel-corrected unit magnifier which was composed of a single lens and concave mirror. It was to be used to project groups of lines for emulsion photography and also phase contrast microscopy. Mertz also proposed the Dyson principle in the same paper where he discussed the Offner. Wynne<sup>9</sup> proposed a Dyson design for microlithography in the visible and ultraviolet and Mouroulis<sup>10,11</sup> et al. considered Dyson designs for visible spectrometry and for coastal ocean applications. A thorough treatment of these designs as well as a working infrared system is described in work by Warren et al<sup>12</sup>. Kuester<sup>13</sup> et al. discuss an airborne platform which uses a visible transmitting Dyson.

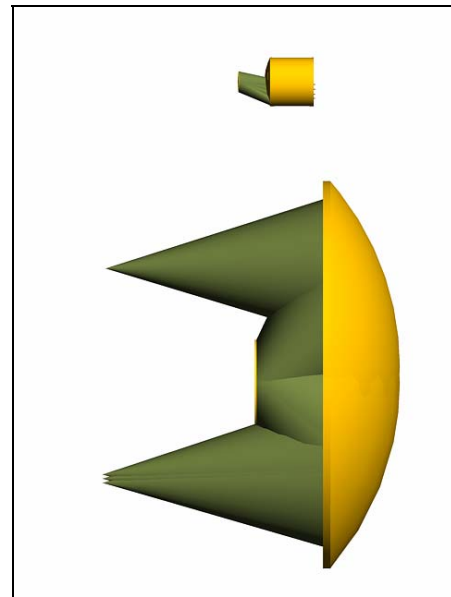


**Figure 1.** Larger Offner (bottom) and smaller Dyson (top) designs for comparable F/#'s and slit width.

Our effort uses the same principle but extends the Dyson design to work optimally with the LWIR. The savings in physical size for similar F/# systems is dramatic as shown in Figure 1. QWEST was designed to minimize smile and keystone distortion<sup>14</sup> while simultaneously virtually eliminating ghosting. The slit width is two detector pixels. Smile and keystone distortions were kept to no more than 1-2% of this or  $\sim 2\mu\text{m}$ . JPL can fabricate ultra precision slits using reactive ion etching which can be kept straight to an order of magnitude better than this [Figure 2]. For this reason the slit straightness is not typically the limiting factor in spectrometer performance. As shown in Figure 2, a single monolithic block is used in double pass where light from the slit enters at a narrow optical passageway and is transmitted through the rear power surface, diffracts off the grating and re-enters the block to totally internally reflect off the back surface which guides the spectrally dispersed radiation to

focus at the QWIP location. This design minimizes the travel and form factor of the system. The actual block fabricated is shown in Figure 3. Broadband area coatings are used on all applicable light transmitting surfaces. The coatings allow 99.5% or better LWIR light to transmit. The block was fabricated from ZnSe, a robust material with a transparent wavelength region from  $0.4 \sim 23 \mu\text{m}$  and an absorption coefficient between  $10^{-3}\text{cm}^{-1}$  and  $10^{-4}\text{cm}^{-1}$ . The ZnSe slab is produced by chemical vapor deposition.

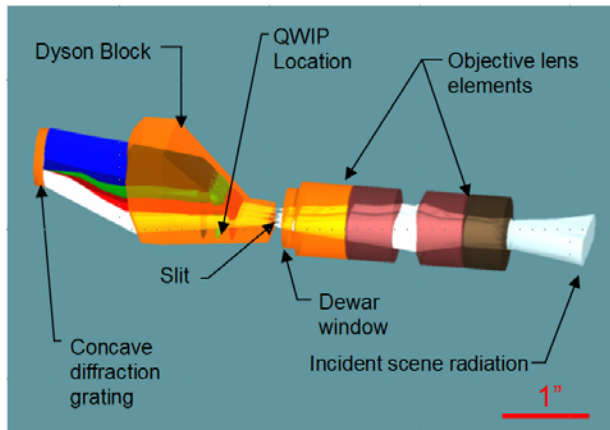


**Figure 2.** Conceptual layout of Dyson spectrometer and objective lens elements

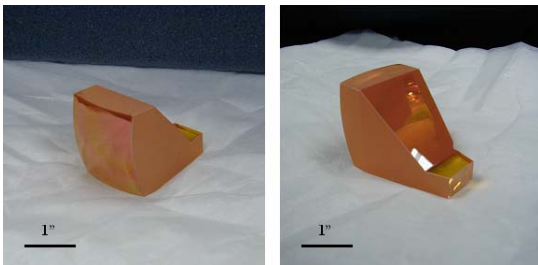


**Figure 3.** Monolithic ZnSe optical block with BBAR coatings used in double pass for the Dyson spectrometer

### 3. THE QWIP ARRAY

QWIP technology<sup>15,16,17</sup> utilizes the photoexcitation of electrons between the ground state and the first excited state in the conduction band quantum well (QW). QWIPs have been successfully integrated into commercial handheld field units for more than a decade. This is the first integration of the QWIP with a spectrometer system for earth science studies requiring accurately calibrated data.

The detector pixel pitch of the FPA is  $25 \mu\text{m}$  and the actual pixel area is  $23 \times 23 \mu\text{m}$ . Indium bumps were evaporated on top of the detectors for hybridization with a silicon readout integrated circuit (ROIC). These QWIP FPAs were hybridized (via indium bump-bonding process) to a  $640 \times 512$  pixel complementary metal-oxide semiconductor

(CMOS) ROIC and biased at  $V_B = -1.25 \text{ V}$ . At temperatures below 72 K, the signal-to-noise ratio of the system is limited by array non-uniformity, readout multiplexer (i.e., ROIC) noise, and photocurrent (photon flux) noise. At temperatures above 72 K, the temporal noise due to the dark current becomes the limitation. We are currently running the system at 40K to have a SNR advantage. The QWIP is known for its high spatial uniformity ( $<0.51\%$ ). This is a clear advantage over other detector technologies such as HgCdTe and InSb. A custom made LCC and titanium FPA clamp was designed to accommodate the close proximity ( $\sim\text{mm}$ 's) of the FPA with the ZnSe block as shown in Figure 4.

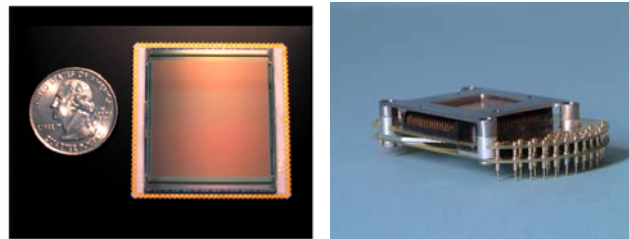
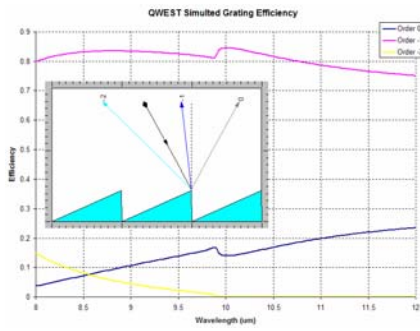


**Figure 4.** QWIP and custom made clamp assembly to hold QWIP and leadless chip carrier (LCC)

### 4. DIFFRACTION GRATING

Diffraction grating design and fabrication is a key enabling technology for these spectrometers. JPL has developed electron-beam lithography techniques that allow fabrication of precisely blazed gratings on curved substrates having several millimeters of height variation.<sup>18,19,20</sup> Gratings fabricated in this manner provide high efficiency combined with low scatter. The blazed grating for this LWIR Dyson spectrometer was fabricated in a thin layer of PMMA electron-beam resist coated on a diamond-turned concave ZnSe substrate. After exposure and development to the desired blaze angle, the resist was overcoated with gold for maximum infrared reflectance. A photograph of the grating and the simulated efficiency of the fabricated grating are shown in Figure 5. The design was optimized for maximum efficiency in the -1 order, and the other orders remain relatively weak across the band. The grating in correct system orientation is shown in figure 6.





(b)

**Figure 5.** QWEST spectrometer grating: (a) photograph of fabricated grating (annular E-beam focus zones are visible due to slight variation in scattering; unexposed rectangular areas near edge are due to the E-beam mount), (b) simulated efficiency (calculated using PCGrate 6.1 software).

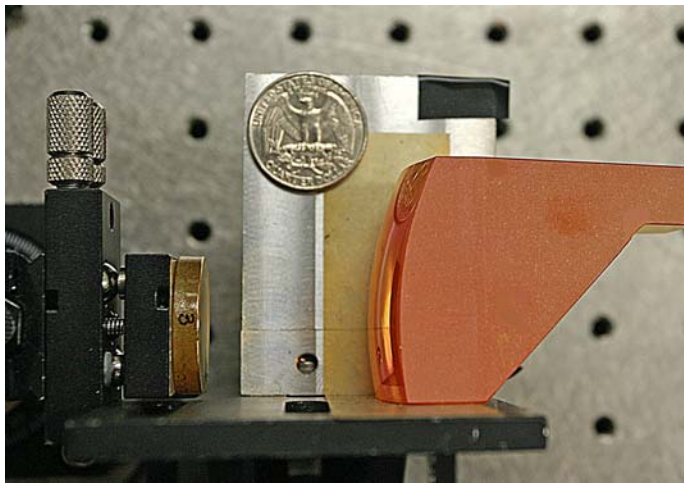


**Figure 6.** Test set-up showing ZnSe block and concave diffraction grating. A U.S. quarter (diameter ~24 mm) is shown for size comparison.

**5. SYSTEM SPECIFICATIONS AND RESULTS**

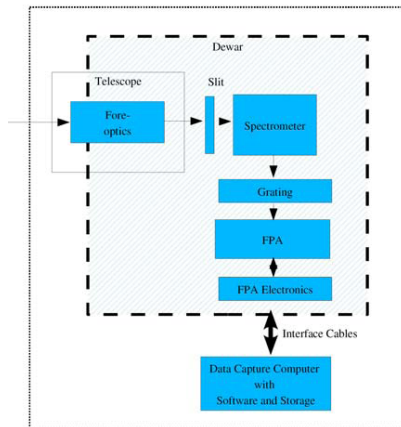
The main goal of this effort was to show as a proof of concept that high quality data can be obtained using the combination of Dyson spectrometer with QWIP detector. Total system isolation from stray light past the spectrometer slit was established by cryogenically cooling all opto-mechanical structures to 40K. This is reasonable due to the small form factor of the system. Currently, stray light analysis using FRED (Photon Engineering, LLC) is being performed to assess further direction in design for HyTES.

First light data reductions are presented for QWEST and look very promising. Excellent spectral signal linearity as well as spectral noise equivalent delta temperature (NEdT) are observed for the peak QWIP sensitivity region surrounding 8.3μm while these response characteristics over the entire band are very reasonable considering the QWIP quantum efficiency (QE) fall-off on either side.

The basic specifications of QWEST and HyTES are shown in Figure 7a with a schematic of the instrument in Figure 7b. Both systems will use large format detectors and have large spatial swath widths. The current optical design and grating works for the entire 8-12μm regime but the existing QWIP FPA which is being used for preliminary testing in QWEST is only sensitive from 8-9μm. The broadband QWIP installation is currently underway and results will be presented in future publications. The close proximity of all electro-optical components can be appreciated in Figure 8. This shows the ZnSe block and hardware in nearly its final configuration.

Instrument Characteristic	QWEST	HyTES
Number of pixels x track	320	512
Number of bands	256	256
Spectral Range	8-12 μm	7.5-12 μm
Integration time (1 scanline)	30 ms	30 ms
Total Field of View	40 degrees	50 degrees
Calibration (preflight)	Full aperture blackbody	Full aperture blackbody
QWIP Array Size	640x512	1024x512
QWIP Pitch *	25 μm	19.5
QWIP Temperature	40K	40K
Spectrometer (Dyson) temperature	40K	40K
Slit Width	50 μm	39 μm
Pixel size at 2000 m flight altitude	4.5 m	3.64
Pixel size at 20,000 m flight altitude	45 m	36.4

a)



b)

**Figure 7.** a) Final system specifications for QWEST and expected for HyTES and b) schematic concept of Dyson spectrometer



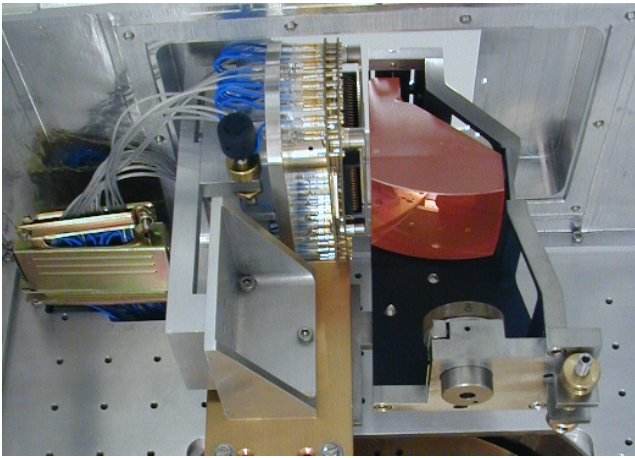


**Figure 8.** Dyson spectrometer testbed in dewar environment.

A spectral calibration was performed using narrowband interference filters. This is an easy way to determine the position of the spectral bands and verify the full width at half maximum. Measured Gaussian filter functions are shown in Figure 9. For radiometric performance, a NIST traceable transfer calibration is performed on our electro-optic blackbody to verify its performance between the two end bracket temperatures of 5C and 30C. JPL has multiple NIST traceable blackbodies with a stability at 25 C of +/- 0.0007 C and a thermistor standard probe with an accuracy of 0.0015 ° C over 0-60 ° C and stability/yr of 0.005. A transfer calibration of the NIST traceable blackbody with the one used for the tests was performed in a ramp and soak mode where the blackbody temperature is increased by a set interval and allowed to soak for several minutes and then the temperature is measured.

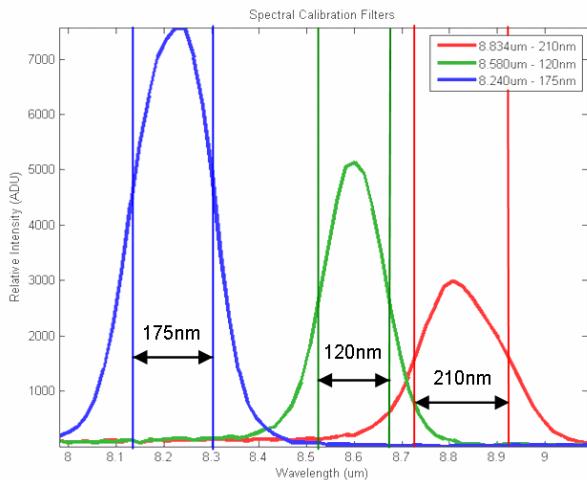
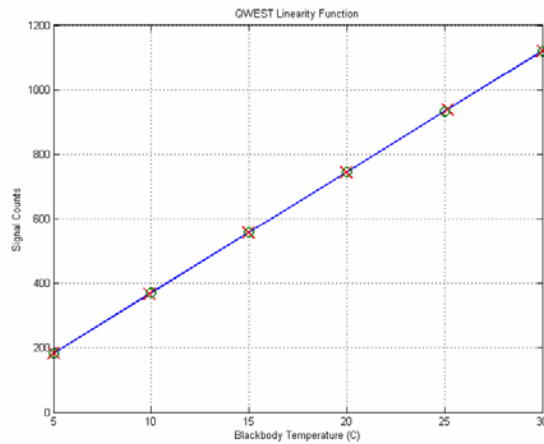


**Figure 9.** Narrowband spectral calibration filter response.

We use a 2-point non-uniformity correction<sup>21,22,23</sup> where 5C and 30C are used to bracket the temperature range. The blackbody is ramped from 5C to 30C and then is left to drift in 5C increments to finally end up back at 5C. Frames are taken at each interval to check for both temporal artifacts as

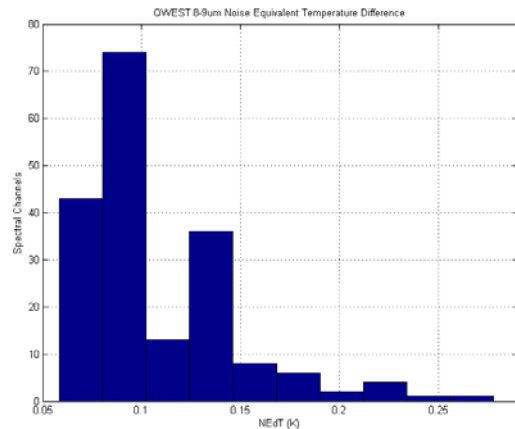
well as single frame noise equivalent temperature difference per spectral band as well as determining any spectral non-linearity.

Two tests were performed to characterize the instrument performance. Test one was for spectral linearity while the other determined the spectral noise equivalent delta temperature (NEdT). Figure 10 shows that QWEST has very good linearity with many temperature measurements showing absolute errors below 0.1C. Figure 10 shows the noise equivalent delta temperature for spectral channels at blackbody temperatures between 5C and 30C. This implies that for a given temperature between this range QWEST has a mean NEdT of 124.7mK.



Actual T	Measured T	Abs. error T
5	5.00	0
10	9.90	-0.1044
15	14.96	-0.0445
20	19.98	-0.0213
25	25.14	0.1354
30	30.00	0

**Figure 10.** Basic QWEST linearity (l.) chart plotted with respect to straight line, (r.) actual readings and absolute error.



**Mean Spectral NEdT: 124.7mK**

**Figure 11.** Noise equivalent temperature difference. The distribution is shown for all spectral channels irrespective of blackbody temperature measured. Measurements were made for a calibrated blackbody between 5C and 30C.

A room-temperature piece of known polyethylene was placed in front of a cold (dark) blackbody and imaged with QWEST indoors. This was done to measure the emission from the known polyethylene source. It also allows understanding of how QWEST radiometric characterization translates into real data. The raw data is divided by a calibrated blackbody at some temperature. Figure 12 shows the derived emissivity relative to the blackbody. Some slight bloating is found of the peak near 8 $\mu$ m of the spectral emissivity response function, and this is attributed to a slight defocus error of the instrument spectral response function.

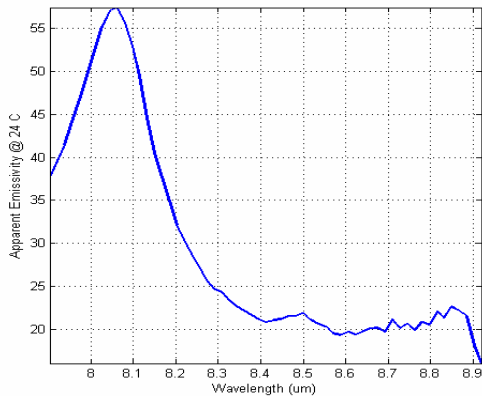


**Figure 12.** Emissivity spectra from miscellaneous polyurethane source

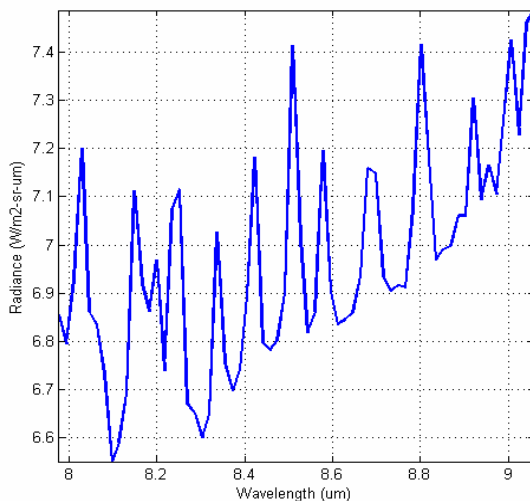


**Figure 13.** Radiance of gold standard with superimposed atmospheric bands as measured in direct sunlight.

The current system is being operated outdoors under direct sunlight to understand and characterize the science usefulness of the instrument towards remote sensing earth science applications. The data shown is using an integration time of 30ms and observed at roughly noon time (Pacific Standard Time). Figure 13 shows radiance calculated for a gold standard. This plot shows atmospheric water band absorption and appears to be both spectrally and radiometrically accurate.

This data is then used in part to further reduce data taken with the system of mineral samples in direct sunlight. As shown in Figure 14, the emissivity spectrum of Quartz sand can be recovered which is in good agreement with previously taken data<sup>24</sup>.

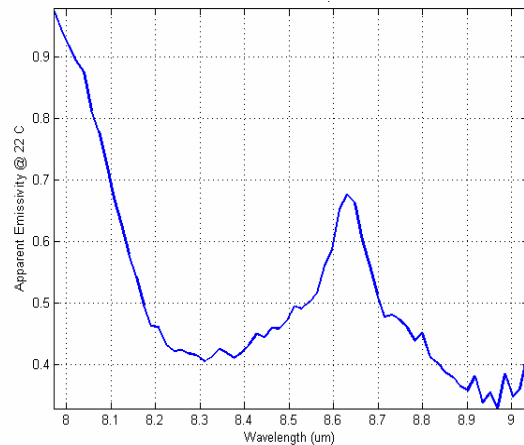


**Figure 14.** Apparent emissivity of quartz as measured by QWEST in direct sunlight.

## 6. REMARKS

A small form factor long wave infrared Dyson spectrometer using a QWIP focal plane array has been demonstrated. The main advantage of the QWIP technology is its excellent spatial uniformity (< 0.5%). Preliminary results show measured NE $\Delta$ T and linearity are excellent. The same spectrometer performance over the nominal LWIR bandpass (8-12 $\mu$ m) is expected once the broadband QWIP installation is completed. Future effort will start to optimize the system using alignment techniques (both cold in rotation and using temperature cycles) to achieve required smile and keystone performance, install the broadband 8-12 $\mu$ m QWIP focal plane array, perform field work to support the earth science testbed effort and begin the transition to a cryocooler airborne instrument.

Strain-layer super lattice detectors<sup>25</sup> which are also being fabricated at JPL have the potential of offering similar uniformity but with a higher operating temperature and higher QE. Future Dyson platform may be able to take advantage of this technology as well.

## 7. ACKNOWLEDGEMENTS

We would like to thank the AVIRIS team (R. Green, M. Eastwood, M. Hernandez, C. Kurzweil, M. Dudick, P. Gardner) for their assistance as well as others associated with the project including Victor White (slit design and production) and SE-IR. This research was carried out at the Jet Propulsion Laboratory, California Institute of Technology, under a contract with the National Aeronautics and Space Administration. Reference herein to any specific commercial product, process, or service by trade name, trademark, manufacturer, or otherwise, does not constitute or imply its endorsement by the United States Government or the Jet Propulsion Laboratory, California Institute of Technology.

## REFERENCES

- [1] <http://moonmineralogymapper.jpl.nasa.gov/>
- [2] <http://aviris.jpl.nasa.gov/>
- [3] A. Offner, "Unit power imaging catoptric anastigmat", U.S. Patent No. 3,748,015 (1973)
- [4] Convex Diffraction Grating Imaging Spectrometer, Patent # 5,880,834, M. P. Chrisp
- [5] L. Mertz, "Concentric spectrographs," *Appl. Optics* 16, 3122-3124 (1977).
- [6] D. Kwo, G. Lawrence, and M. Chrisp, "Design of a grating spectrometer from a 1:1 Offner mirror system," *SPIE Proc.* 818, 275-279 (1987)
- [7] D. R. Lobb, "Theory of concentric designs for grating spectrometers," *Appl. Optics* 33, 13, 2648-2658 (1994)
- [8] J. Dyson, "Unit Magnification Optical System without Seidel Aberrations," *Journal of the Optical Society of America*, Vol. 49, No. 7, 713-716, 1959.
- [9] C. G. Wynne, "Monocentric telescopes for microlithography," *Opt. Eng.* 26, 300-303 (1987)
- [10] P. Mouroulis and R. O. Green, "Optical design for imaging spectroscopy," *Proc. SPIE* 5173, 18-25 (2003)
- [11] Pantazis Mouroulis, Robert O. Green, and Daniel W. Wilson *Optics Express*, Vol. 16, Issue 12, pp. 9087-9096  
Optical design of a coastal ocean imaging spectrometer
- [12] David W. Warren; Dan A. Gutierrez; Eric R. Keim, "Dyson spectrometers for high-performance infrared applications," *Optical Engineering* 47(10), 103601
- [13] Michele A. Kuester, James K. Lasnik, Tanya Ramond, Tony Lin, Brian Johnson, Paul Kaptchen, William Good, Earth Observing Systems XII, edited by James J. Butler, Jack Xiong, *Proc. of SPIE Vol.* 6677, 667710, (2007)
- [14] P. Mouroulis, R. O. Green, and T. G. Chrien, "Design of Pushbroom Imaging Spectrometers for Optimum Recovery of Spectroscopic and Spatial Information," *Applied Optics*, Vol. 39, No. 13, 2210-2220, 1 May 2000.
- [15] S. D. Gunapala, S. V. Bandara, J. K. Liu, S. B. Rafol, and J. M. Mumolo, "Large Format Multiband QWIP Focal Plane Arrays," in *Infrared Spaceborne Remote Sensing XI*, Marija Strojnik, eds., *Proc. of SPIE Vol.* 5152, pp. 271-278, Nov. 2003.
- [16] S. D. Gunapala, S. V. Bandara, J. K. Liu, C. J. Hill, S. B. Rafol, J. M. Mumolo, J. T. Trinh, M. Z. Tidrow, and P. D. LeVan, "Multicolor megapixel QWIP focal plane arrays for remote sensing instruments," in *Photonics for Space Environments XI*, Edward W. Taylor eds., *Proc. of SPIE Vol.* 6308, pp. 63080P, Sep. 2006.
- [17] S. D. Gunapala, S. V. Bandara, J. K. Liu, J. M. Mumolo, C. J. Hill, E. Kurth, J. Woolaway, P. D. LeVan, and M. Z. Tidrow, "Towards Dualband Megapixel QWIP Focal Plane Arrays," in *Infrared Technology and Applications XXXIII*, Bjørn F. Andresen, Gabor F. Fulop, Paul R. Norton eds., *Proc. of SPIE Vol.* 6542, May 2007.
- [18] P. D. Maker, R. E. Muller, and D. W. Wilson, "Diffractive optical elements on non-flat substrates using electron beam lithography," US Patent. No. 6,480,333, assigned to California Institute of Technology, Pasadena, CA (1998).
- [19] D. W. Wilson, P. D. Maker, R. E. Muller, P. Z. Mouroulis, and J. Backlund, "Recent advances in blazed grating fabrication by electron-beam lithography", *Proc. SPIE Vol.* 5173, pp. 115-126 (2003).
- [20] D. W. Wilson, R. E. Muller, P. M. Echternach, and J. P. Backlund, "Electron-beam lithography for micro- and nano-optical applications," *Proc. SPIE Vol.* 5720, pp. 68-77 (2005).
- [21] D. L. Perry and E. L. Dereniak, "Linear theory of nonuniformity correction in infrared staring sensors," *Opt. Eng.* 32, 1853-1859 (1993)

- [22] A. E Milton, E R. Barone, and M. R. h e r , “The influence of nonuniformity on IR focal plane may performance,” in Second Conference on Advanced IR Detectors and Sys.rems, 1983.
- [23] J. M. Mooney, E D. Shepard, W. S. Ewing, J. E. Murguia and J. Silverman, “Response nonuniformity limited performance of infrared staring cameras,” Optical Engineering, vol. 28, pp 1151-1161, November 1989.
- [24] S. J. Hook, A. B. Kahle, “The Micro Fourier Transform Interferometer,” Remote Sensing Environment, Elsevier Science, 56:172-181.
- [25] Cory J. Hill; Jian V. Li; Jason M. Mumolo; Sarath D. Gunapala; David R. Rhiger; Robert E. Kvaas; Sean F. Harris, MBE grown type-II superlattice photodiodes for MWIR and LWIR imaging applications, Proceedings Vol. 6542, Infrared Technology and Applications XXXIII, Bjørn F. Andresen; Gabor F. Fulop; Paul R. Norton, Editors, 654205Date: 14 May 2007.